Optical and Quantum Electronics (2023) 55:514
https://doi.org/10.1007/s11082-023-04797-7

New Sb_2Se_3-based solar cell for achieving high efficiency theoretical modeling

Abdelaziz Ait Abdelkadir[1] · Mustapha Sahal[1] · Essaadia Oublal[1] · Naveen Kumar[2] · Abdellah Benami[3]

Received: 23 August 2022 / Accepted: 23 March 2023 / Published online: 8 April 2023

Abstract
In this paper, we presented a numerical study of a CdS/Sb_2Se_3 mono junction solar cell (**SC**) using the **SC** Capacitive Simulator (SCAPS-1D). We validated an experimental work using a variety of Sb2Se3 experimental parameters, and the results showed excellent agreement between numerical and experimental J-V curves, yielding a PCE of 7.54%.To continue, we analyzed the impact of Sb_2Se_3 thin layer thickness, charge carrier concentration, bulk defect density, and interface defect (CdS/Sb_2Se_3) on solar cell characteristics. With the optimum Sb2Se3 layer thickness of 1.2 µm, carrier concentration of 10^{15} cm^{-3}, bulk defect of 10^{13} cm^{-3}, and CdS/Sb2Se3 interface defect densities of 10^{10} cm^{-2}, we were able to attain an efficiency of 16.62%, Jsc = 35.38 mA/cm^2, Voc = 0.66 V, and FF = 70.33%. Finally, we investigated the insertion effect of n-GaAs (ETL) and P^+-CuO HTL (BSF) on Sb_2Se_3 solar cell efficiency. The novel ITO/n-CdS/n-GaAs/p-Sb_2Se_3/p^+-CuO HTL/Au heterostructure achieved a huge efficiency of 19.60%.

Keywords Solar Cell · Sb_2Se_3 · n-GaAs · P^+-CuO HTL B.S.F · 19.60% efficiency

1 Introduction

Recently, it has become clear that we must use energy transformation to improve the quality of life and increase productivity by providing access to renewable energy, which is a critical aspect of socioeconomic growth and development. In light of this, solar cell (SC) systems and thin films have received significant scientific attention and have proven commercially successful. PV materials are engineered to meet challenges such as high energy

✉ Abdelaziz Ait Abdelkadir
abdelazizaitabdelkadir@gmail.com

✉ Mustapha Sahal
sahalmustapha@gmail.com

[1] MESE/Lab. PETI, Ouarzazate Polydisciplinary Faculty, University of Ibn Zohr, Agadir, Morocco

[2] Department of Chemistry, Maharshi Dayanand University, Rohtak, Haryana, India

[3] LM3ER-OTEA Department of Physics, Faculty of Sciences and Techniques, Moulay Ismail University of Meknes, BP 509, 52000 Boutala-Mine, Errachidia, Morocco

conservation, competitive prices, easy fabrication processes, and long-term longevity and stability. Several types of solar cells (SCs), including CdTe (Ahmed et al. 2020), the kesterite family (Bouarissa et al. 2021), CIGS (Biplab et al. 2020), perovskite (Jannat et al. 2021), and the family of antimony chalcogenide binary compounds (Sb_2X_3) (Dong et al. 2021), have been extensively researched in the literature due to their optimum gap, strong absorption coefficients in the visible spectrum range as well as excellent power conversion efficiency (PCE). In this context, chalcogenide antimony selenide Sb_2Se_3 (orthorhombic structure) has been recognized, as a potential SC due to its poor toxicity, low cost, earthly abundance, high electrical conductivity, strong absorption coefficient ($> 10^5$ cm^{-1}), and appropriate energy band gap (1.03 eV indirect and 1.17 eV direct), which is close to the optimal Shockey-Queisser value (Dong et al. 2021). Although, the highest Sb_2Se_3 thin layer SCs PCE with a CdS/Sb_2Se_3 superstrate and a $CdS/TiO_2/Sb_2Se_3$ substrate configuration are currently 7.6% (Wen et al. 2018) and 9.2% (Spalatu et al. 2021) respectively. This experimental efficiency remains lower than that of the other semiconductor SCs. Nevertheless, the open-circuit voltage (V_{oc}) of the Sb_2Se_3 SC is undoubtedly small, with values ranging from 0.3 to 0.5 V attributed to bulk recombination leakage, interfaces, and back contact recombination loss, implying a large space for approaching its theoretical thermodynamic limit (0.9 V for an E_g of 1.2 eV) (Liang et al. 2020). To date, in order to fabricate a good CdS/Sb_2Se_3 device, different film deposition methods have been utilized to improve their quality and electronic properties, such as thermal evaporation (Cang et al. 2020), vapor transporting deposition (VTD) (Tao et al. 2019), magnetron sputtering (Tang et al. 2019), and solution processing (Zhou et al. 2014). Using interdiffusion layers (ETL) such as TiO_2 (Spalatu et al. 2021) at the CdS/Sb_2Se_3 interface provides one of the opportunities to eliminate the diffusion of Se and Sb to CdS, reducing interface defect formation and improving the Sb_2Se_3-based SC.

To improve the performance of Sb_2Se_3 SCs, we propose using the SCAPS-1D to analyze and optimize the ITO/CdS/Sb_2Se_3/Au SC characteristics. We then fit and validate Sb_2Se_3 experimental J-V characteristics using the available experimental parameters, resulting in a strong agreement between experimental and theoretical simulations (PCE = 7.54%, J_{sc} = 29.25 mA/cm^2, V_{oc} = 0.44 V, and FF = 58.28%), demonstrating that the SCAPS -1D program is perfect program for describing and developing Sb_2Se_3-based SC characteristics. Following that, we investigated the effects of Sb_2Se_3 film width, carrying capacity, defect density, the insertion of n-GaAs as a second buffer, and CuO HTL as a BSF on several recombination losses and efficiency. The novel combination ITO/n-CdS/n-GaAs/p-Sb_2Se_3/p^+-CuO (HTL)/Au achieved an excellent efficiency of 19.60%, a V_{oc} of 0.73 V, a J_{sc} of 36.38 mA/cm^2, and a FF of 73.47%, which may encourage the experimental laboratory to produce the same configuration.

2 Material parameters and device architecture

2.1 Symbols

Ψ	Electrostatic potential.
ε^0	Vacuum permittivity.
ε_r	Semiconductor permittivity.
n and p	Free carrier concentrations.

N_d^+	Ionized donor density.
The great	Acceptor density.
"ρdef"	Defect charge density.
G	Generation rate.
j_n	Electron current density.
j_p	Hole current density.
q	Elementary charge.
U_n	Electrons recombination rate.
U_p	Holes recombination rate
μ_p	Holes mobility.
μ_n	Electrons mobility.
HTL	Hole Transport Layer
BSF	Back-surface field.
E_g	Energy band gap.
χ	Electron affinity.
ε	Dielectric permittivity,
NC	Conduction band states density.
NV	Valence band states density.
V_{thn} and V_{thp}	E^- and p^+ hole thermal velocity.
ETL	Electron transport layer.
R_s	Series resistance.
R_{sh}	Shunt resistance

The SCAPS-1D software developed by Gent University in Belgium (Burgelman and Marlein 2008) was largely used to theoretically describe and analyze SC devices by solving semiconductor equations such as the Poisson, the continuity equations for electrons, the continuity equations for holes (1,2,3), as well as drift and diffusion Eqs. (4, 5).

$$\frac{\partial}{\partial x}(\varepsilon^0 \varepsilon_r \frac{\delta}{\delta x}) = -q\left(p - n + N_d^+ - N_A^- + \frac{\rho def}{q}\right) \tag{1}$$

$$-\frac{\partial j_n}{\partial x} - U_n + G = \frac{\partial n}{\partial t} \tag{2}$$

$$-\frac{\partial j_p}{\partial x} - U_p + G = \frac{\partial p}{\partial t} \tag{3}$$

$$j_n = -\frac{U_n n}{q}\frac{\partial E_{Fn}}{\partial x} \tag{4}$$

$$j_p = +\frac{U_p p}{q}\frac{\partial E_{Fp}}{\partial x} \tag{5}$$

In this paper, we are interested in the analysis and development of the optoelectronic performance of the Sb_2Se_3 SC via SCAPS-1D. Note that SCAPS-1D is a simulation tool with seven semiconductor layers of input from which we can compute the effect of several electronic parameters. The physical parameters of the SC device that have

been taken into account in the simulation environment (1.5 air mass spectrums, ambient temperature of 25 °C, and 100 mW/cm^2 sun illuminations) were recorded from experimental measurements and other scientific papers and are shown in Tables 1, 2, 3, and 4.

Table 1 Back and front grid parameters

Parameters	Front metal contact	Back metal contact
Metal work function $\varphi\,(eV)$	Flat	Au
S_e (cm/S)	10^7	10^7
S_h (cm/S)	10^7	10^7

Table 2 Optimized parameters that were employed in the ITO/CdS/Sb_2Se_3/CuO HTL/Au hetero-junction device simulation

Parameters	P^+-CuO HTL (Khattak et al. 2019)	Sb_2Se_3 (Baig et al. 2020)	n-GaAs (Khan and Khan 2018)	CdS (Abdelkadir et al. 2022a)	ITO (Oublal et al. 2022)
Thickness (nm)	100	1200	100	70	100
E_g (eV)	2.2	1.19	1.43	2.42	3.6
χ (eV)	3.2	4.18	4.07	4.4	4.5
ε_r	7.1	14.5	12.9	10	8.9
N_C (cm^{-3})	2.5×10^{18}	2×10^{18}	2.2×10^{18}	1.2×10^{18}	2.2×10^{18}
N_V (cm^{-3})	1.5×10^{19}	1×10^{19}	1.8×10^{19}	1.8×10^{19}	1.8×10^{19}
μ_N (cm^2/v.s)	200	16.70	8500	100	10
μ_P (cm^2/v.s)	800	16.70	400	50	10
$N_D(cm^{-3})$	0	0	1×10^{11}	2.1×10^{17}	10^{21}
N_A (cm^{-3})	5×10^{21}	2×10^{16}	0	0	0
Radiative recombination coefficient (cm^3/s)	2.3×10^{-9}	2.3×10^{-9}	2.3×10^{-9}	–	–

Table 3 The interfaces parameters utilized in this work

Parameter	CdS/Sb_2Se_3	Sb_2Se_3/CuO HTL
Defect nature	Neutral	Neutral
Electrons capture cross section	10^{-16}	10^{-16}
Holes capture cross section	10^{-16}	10^{-16}
Reference for defect energy level E_t	above the highest Ev	
Energy with respect to Reference (eV)	0.06	0.06
Total density (Nt)	10^{11}	10^{10}

Table 4 The materials' defect input that was used in this simulation

Defects properties	ITO (Oublal et al. 2022)	CdS/GaAs (Oublal et al. 2022)	Sb_2Se_3 [SCAPS]	CuO HTL(Khattak et al. 2019)
Defects density N_t (cm^{-3})	0	$A : 10^{17}$	$D : 3.10^{14}$	$D : 10^{15}$
σ_n (cm^2)	–	10^{-17}	4.10^{-13}	10^{-14}
σ_p (cm^2)	–	10^{-13}	4.10^{-13}	10^{-14}
$E_A or E_D$(eV)	Medium of the gap			
Defect type	–	Single acceptor	Single donor	Single donor
Energetic distribution		GauB	Single	Single
Reference for defect energy level E_t	Above EV (SCAPS < 2.7)			
Energy level with respect to reference BV	–	0.1	0.6	0.6

3 Results and discussion

3.1 Theoretical analysis of the ITO/CdS/Sb_2Se_3/Au conventionnel solar structure

In this part of the work, we show a numerical investigation and optimization of ITO/CdS/Sb_2Se_3/Au SC through the SCAPS-1D tool. Figure 1 depicts the schema structure and energy band diagram of Sb_2Se_3 hetero-junction SC. As shown, the ITO was employed as the window thin film, CdS as a buffer film, Sb_2Se_3 as an absorber, and Au as the back electrode. It is observed from Fig. 1 that CdS/Sb_2Se_3 has a negative conduction band offset CBO^{-}. This negative sign indicates that the conduction band of CdS is lesser than that of Sb_2Se_3, which may be one of the factors for implying the free flow of electrons, hence minimizing short circuit current and thus affecting SC performance.

a. Validation of Sb_2Se_3 simulated parameters with experimental work

In this first subsection, the experimental parameters of the ITO/CdS/Sb_2Se_3/Au-based SC reported in the work of Xixing WEN et al., such as Sb_2Se_3 layer thickness (0.9 μm),

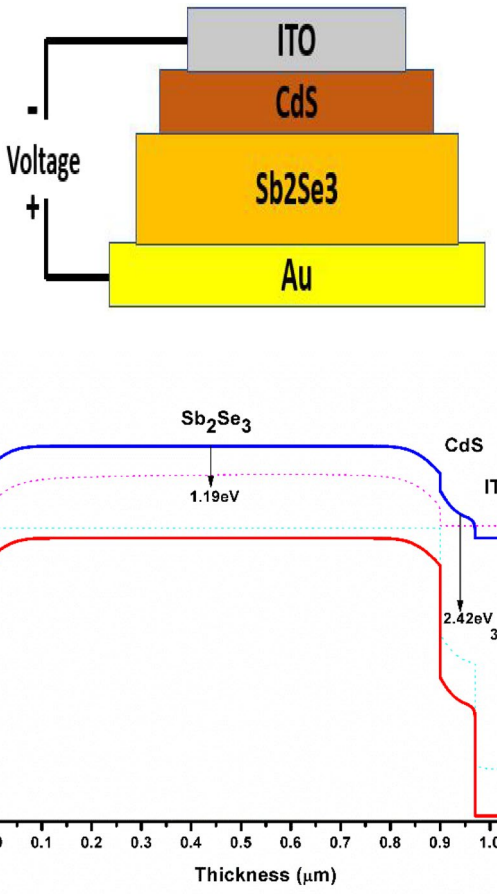

Fig. 1 The configuration and band diagram of the Sb_2Se_3 conventional SC

carrier concentration (2.10^{16} cm^{-3}), and interface defect (2.10^{11} cm^{-2}) with other parameters shown in Tables 1, 2, 3, and 4**,** are collected and fed into SCAPS-1D software. Xixing et al. (Wen et al. 2018) used vapor transport deposition of antimony selenide thin film solar cells at various heating temperatures, pressures, and substrate temperatures to analyze the crystallinity evolution and fabricate high-quality solar cells with a PCE of 7.6%, a V_{OC} of 0.42 V, a J_{SC} of 29.9 mA/cm^2, and a FF of 60.4%.

At 2.10^{14} cm^{-3} in Sb_2Se_3 defect density, we found a strong agreement between the experimental (Wen et al. 2018) and theoretical J-V curves (see Fig. 2), resulting in a PCE of 7.54%, a V_{OC} of 0.44 V, a J_{SC} of 29.25 mA/cm^2, and a FF of 58.36%. This finding demonstrates the realistic models and the excellence of software used in this work.

b. Impact of Sb_2Se_3 thickness and charges concentration on the conventional SC characteristics.

The absorber film thickness and charge concentration have a significant impact on the carriers generated when photons are incident on solar cell devices. So, after validating the Sb_2Se_3 experimental model with theoretical model one, we start optimizing the Sb_2Se_3 thickness and carrier density (Na) in the 0.2–1.2 µm and 10^{13}–10^{18} cm^{-3} ranges, respectively. The results for quantum efficiency (a) and current density (b) versus Sb_2Se_3 thickness and carrier concentration are shown in Fig. 3a and b, respectively. Figure 3a shows that by increasing the absorber thickness (while keeping the other parameters constant), the quantum efficiency increases and reaches a maximum value at 1.2 µm, which can be explained by collecting the maximum number of photons, resulting in enhanced production of electron–hole pairs**.** As a result, the cell's output will increase, improving the overall efficiency of the Sb_2Se_3 solar cells**.** Figure 3b also depicts the effect of the Sb_2Se_3 carrier concentration density on the J-V properties. It can be seen that J_{sc} increases with acceptor concentration to a maximum at 10^{15} cm^{-3} and decreases with higher concentrations, which is due to the charges recombination rate and impurity scattering, which increase as acceptor carrier concentration increases, reducing carrier collection at the interface and forcing current to be drastically reduced.

Figure 4 shows the evaluation and representation of the dual effects of Sb_2Se_3 acceptor concentration and layer depth on ITO/CdS/ Sb_2Se_3 /Au S.C. characteristics (V_{oc}, J_{sc},

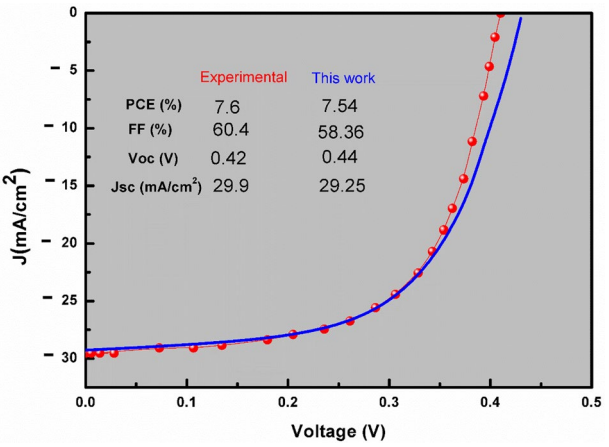

Fig. 2 Comparing J-V features of experimental and simulated conventional solar cell structures (see Fig. 1)

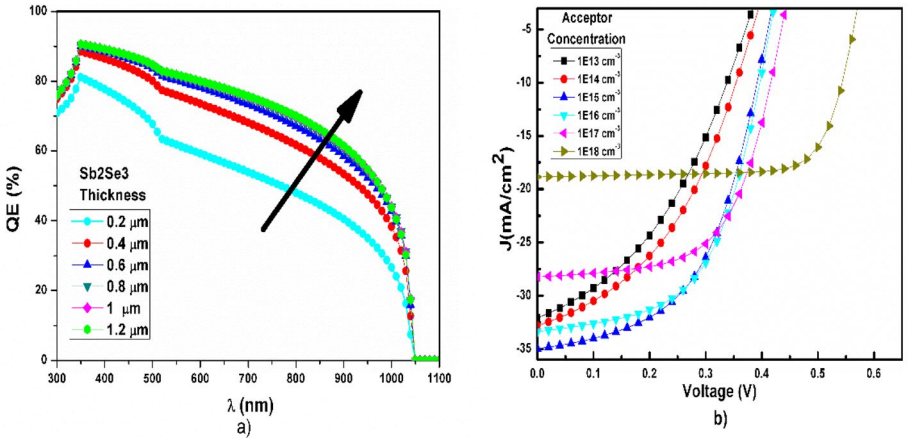

Fig. 3 Sb_2Se_3 thickness and acceptor concentration effect on QE **a** and J–V characteristics **b**

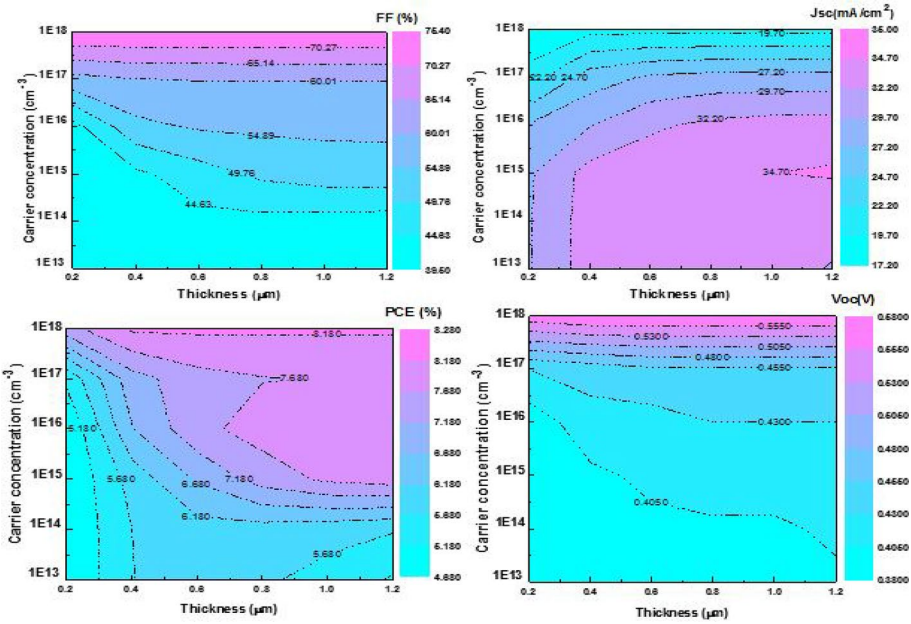

Fig.4 Impact of Sb_2Se_3 thick and charges carrier concentration on the PV characteristics of studied heterostructure

FF, and PCE). The figure shows how the acceptor density of the Sb_2Se_3 changed the S.C. characteristics. Since at high carrier concentrations $> 10^{17}$ cm^{-3}, PCE, FF, and open-circuit voltage, all exhibit good values even at low absorber thicknesses, their maximum values are only attained at thicknesses greater than 0.8 µm. Although J_{sc} behaves differently, the greater long-wavelength photon absorption in this layer can account for the increase in J_{sc} as absorber thickness increases. However, as acceptor carrier concentration increases, the

lifetime of photogenerated electrons shortens, reducing the number of carriers gathered at the interface and thus decreasing J_{sc} (Biplab et al. 2020). As a result, we can see in Fig. 4 that the maximum efficiency was ~ 8.25% with J_{sc} of 18.85 mA/cm^2, FF of 75.33%, and V_{oc} of 0.58 V for thickness and carrier concentration of 1.2 µm and 10^{18} cm^{-3}, respectively. However, in this section, we are interested in achieving a high J_{sc} (35 mA/cm^2), which will result in the creation of more electron pairs and thus higher solar cell efficiency. So, we suggested keeping the carrier concentration density (N_a) at 10^{15} cm^3 and the thickness at 1.2 µm as optimal practical values. The low FF and V_{oc} at these optimal values can be resolved by minimizing traps at recombination centers and interface-induced recombination losses caused by bulk depth carrier trap zones, inappropriate energy-level alignment, mismatched lattice at the interface, and dangling bonds at surface interfaces (Dong et al. 2021); the implications of this will be shown in the following sections.

c. Effect of the Sb_2Se_3 bulk defect density and interfacial defect on conventional Sb_2Se_3 solar cell characteristics

The Sb_2Se_3 bulk defect density and interface defects are critical parameters for designing a high-performance CdS/Sb_2Se_3 photovoltaic cell with low parasitic resistance. The most common intrinsic defects in the Sb_2Se_3 crystal structure are V_{se}, V_{Sb}, Sb_i, Se_i, Sb_{Se}, and Se_{Sb} (Huang et al. 2019). As a result, we proposed analyzing and optimizing this parameter from 10^{10} to 10^{16} cm^{-3} (bulk defect) and from 10^{10} to 10^{16} cm^{-2} (CdS/Sb_2Se_3 interface defect) to minimize higher band bending at the absorber/buffer interface, which is a major impediment to the generated electrons and holes (electrical transport across the junction interface) and bulk charge carrier recombination Figs. 4 and 5 depicts a significant decrease in the three parameters that determine the yield of the Sb_2Se_3 device as bulk and interface defect increase, owing to an increase in trap-assisted Shockley–Read–Hall (SRH), surface recombination velocity, and reduction lifetime. The J_{SC} and FF decrease because electrons are more likely to be captured and device resistance increases, reducing efficiency**.** For ITO/CdS/Sb_2Se_3/Au solar cell with 1.2 µm absorber layer thickness, 10^{15} cm^{-3} carrier concentration, 10^{13} cm^{-3} bulk defect density, and 10^{10} cm^{-2} for CdS/Sb_2Se_3 interface defect density, an optimal efficiency of 16.62%, V_{oc} of 0.66 V, J_{sc} of 35.38 mA/cm^2, and FF of 70.33% was found, which is more promising than the efficiency of the reported article (Cang et al. 2020; Tang et al. 2019; Tao et al. 2019; Zhou et al. 2014). These results provide critical quantitative insights to understand the defect's impact on device performance.

In the next part of this work, we set the Sb_2Se_3 material parameters at their optimal values and discuss the influence of the incorporation of GaAs and CuO HTL interlayers on the device performances.

d. Theoretical Analyzing of ITO/CdS/n-GaAs/Sb_2Se_3/CuO HTL/Au new hetero structure

n this section, we investigate and analyze the effect of n-GaAs and P^+-CuO HTL insertion on the Sb_2Se_3 SC properties. Figure 6 depicts the new hetero SC schematic configuration and band diagram. According to the band diagram, incorporating a thin n-GaAs layer (100 nm) results in a positive and low conduction band offset (CBO), which aids in the free flow of electrons from the absorber layer (p-Sb_2Se_3) to hybrid buffer layers (n-GaAs/n-CdS). Furthermore, WILLIAMS et al. (Williams et al. 2020) demonstrated that CdS is unsuitable as a direct transmitter to the Sb_2Se_3 absorber due to Se and Sb interdiffusion, which is the original cause of the very deficient interface and Sb_2Se_3 absorber layer,

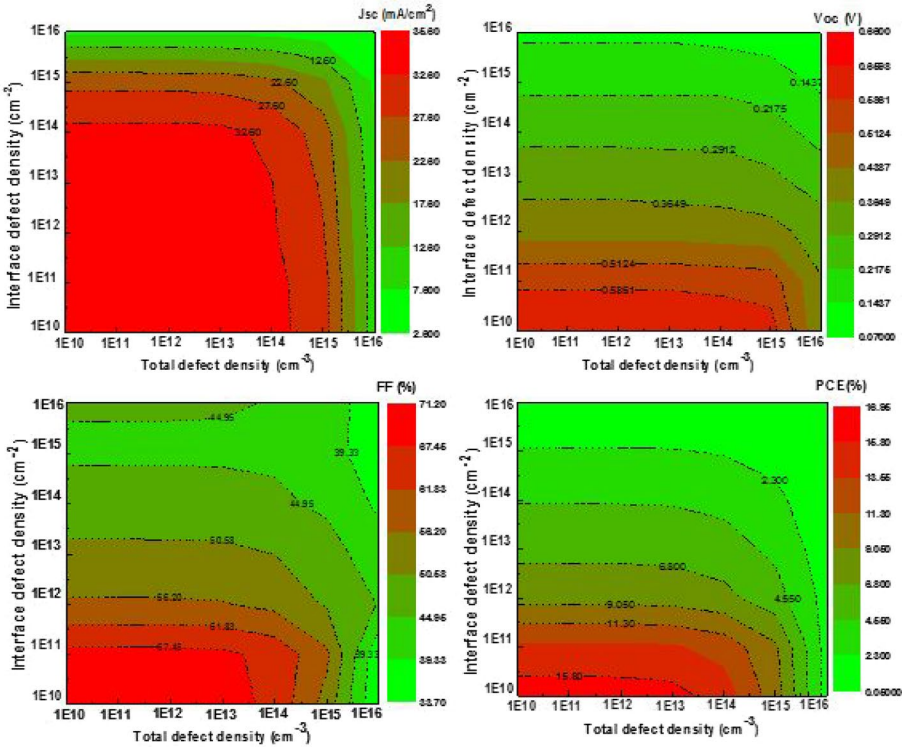

Fig. 5 Impact of Sb_2Se_3 defect on the PV characteristics of studied heterostructure

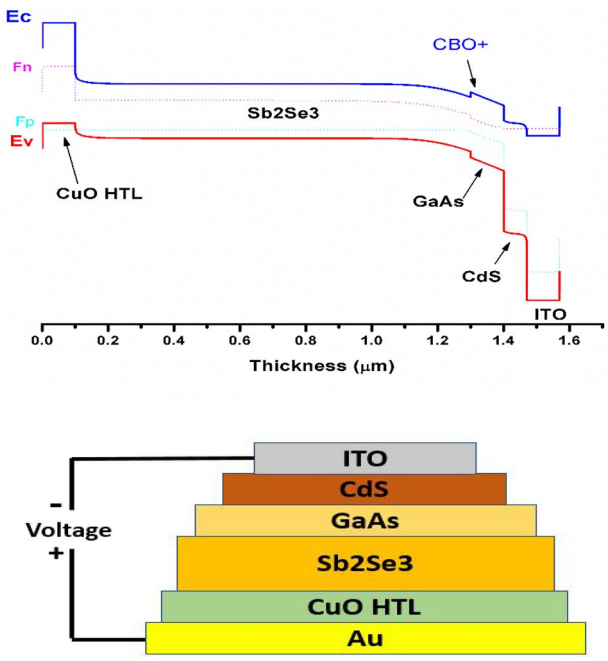

Fig. 6 Optimal Sb_2Se_3 solar cell structure with n- GaAs ETL and p^+- CuO HTL layers

potentially lowering device performance via interface recombination loss. As a result, using a thin layer of n-GaAs can provide the opportunity to fabricate high Sb_2Se_3 SC quality with a low interfacial defect. Moreover, the insertion of CuO HTL creates a high potential barrier at back contact, potentially reducing recombination at this interface.

e. Effect of the incorporation of n- GaAs and P + -CuO HTL interlayers on the Sb_2Se_3 solar cell characteristics

To create a dual-buffer-layered Sb_2Se_3 solar cell, a second buffer layer was added to the first buffer layer, and the parameters were altered by adjusting the thickness ratio, as shown in Fig. 8a. A dual buffer layer is created here by combining n-CdS and n-GaAs. The FF and PCE values were found to be higher than in the single-buffer-layer cases. We observed a positive CBO^+ with an optimum offset of 0–0.4 eV at the n-GaAs/Sb_2Se_3 interface after the addition of n-GaAs (see Fig. 6), indicating that the Sb_2Se_3 absorber is in conjunction with the good buffer layer (n-GaAs), which can yield better efficiencies by lowering interface recombination and selective charge collection.

However, high recombination of electron minority charge carriers at the metal back contact layer gives the chance to boost the SC efficiency due to the possibility of high impurity doping concentration on the back of the solar cell. This can be accomplished by injecting a higher doping concentration into the back-surface field (BSF) layer than the active absorber layer, creating a high potential barrier that can reflect electrons to the P–N junction space (Abdelkadir et al. 2022b; Ait Abdelkadir et al. 2022; Kaminski et al. 2002).

As shown in Fig. 7, using CuO HTL as a back surface field (ITO/CdS/GaAs/Sb_2Se_3/CuO HTL) improves SC quantum efficiency (QE) and current density, which can be explained by the high electric field between the grain boundary and the interior of the grain (Zhou et al. 2014), decreasing carriers at the deep center, and increasing the created electric potential (see Fig. 7c, d). The strong electric field at the interfaces accelerates photogenerated carrier separation at the depletion region, drawing them away from the junction quickly. While the holes pass through the HTL layer and are collected by the rear contact, the electrons travel into the buffer layer. Charge carriers avoid recombination by using band offsets to reach the metal contact (Biplab et al. 2020).

The effect of n-GaAs ETL and P^+-CuO HTL interlayer thickness from 20 to 200 nm on the basic parameters of Sb_2Se_3 SCs, including PCE, V_{oc}, J_{sc}, and FF, were investigated and shown in Fig. 8.

It is clearly noticed in Fig. 8a that the FF grows linearly with the thickness of the n-GaAs thin layer, leading to a rise in PCE. This could be attributed to the formation of a proper depletion region, which reduces interface string resistance and enhances carrier collection. However, a very low decrement of J_{sc} was observed, which could be due to the high radiative recombination coefficient that we take into account in this simulation ($2.3.10^{-9}$), and no significant effect on SC V_{oc} with n-GaAs layer thickness adjustments was observed. The Sb_2Se_3 SC characteristics are saturated with the increment of the CuO HTL thickness at a high efficiency of 19.60% with J_{sc} of 36.38 mA/cm^2, V_{oc} of 0.73 V, and FF of 73.47%. This rise is due to a decrease in charge carrier recombination (Ait Abdelkadir et al. 2022), which improves carrier gathering and increases SC efficiency. As a result, investigators can be more confident in using n-CdS/n-GaAs hybrid buffer layers with CuO HTL as back contact to achieve maximal Sb_2Se_3 device performance. Next, we set the n-GaAs layer thickness to 100 nm and began varying the CuO HTL (BSF) layer thickness from 20 to 200 nm (see Fig. 8b).

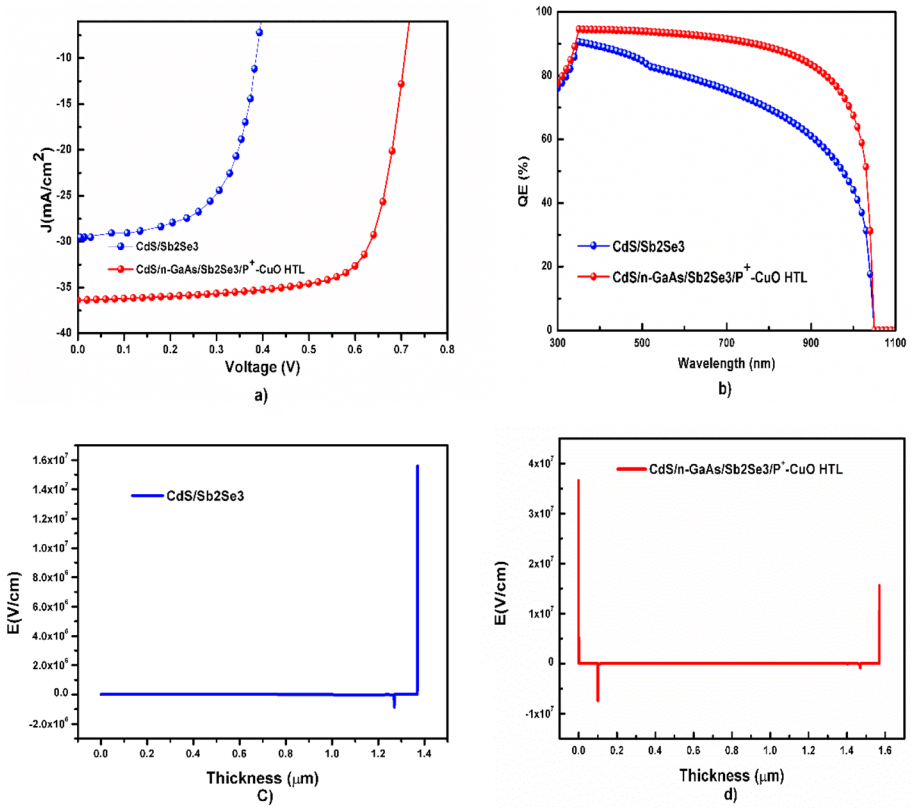

Fig. 7 Current density versus potential (J-V) **a**, Quantum efficiency **b**, and electric field (c and) of the conventional SC and the optimal one

f. Effect of parasitic resistance on new hetero solar cell characteristics

The influence of parasitic resistance on the new hetero SC is also investigated. As illustrated in Fig. 9a, b, augmenting the R_s from 0 $\Omega.cm^2$to 10 $\Omega.cm^2$ causes the J_{SC} and FF to decrease linearly, increasing the SC efficiency inversely to the increase in R_{sh} and thus improving the SC PCE. As a result, for high Sb_2Se_3 SC efficiency, it is necessary to fabricate this dispositive with low R_s and high R_{sh}. Furthermore, we compare the findings of this study to previous studies reported in published research. Table 5 summarizes the comparative studies of current outcomes with some recently published Sb_2Se_3-based SCs. We can see that the outcome of this paper paves the way for higher Sb_2Se_3 SC efficiency.

4 Conclusions

In this paper, SCAPS-1D program was used to validate a theoretical model that describes the experimental Sb_2Se_3 solar cell characteristics. We found that several parameters, including Sb_2Se_3 thin layer thickness, charge carrier concentration, and bulk and interface defects, limit the performance of Sb_2Se_3-based solar cells. The analysis of several features

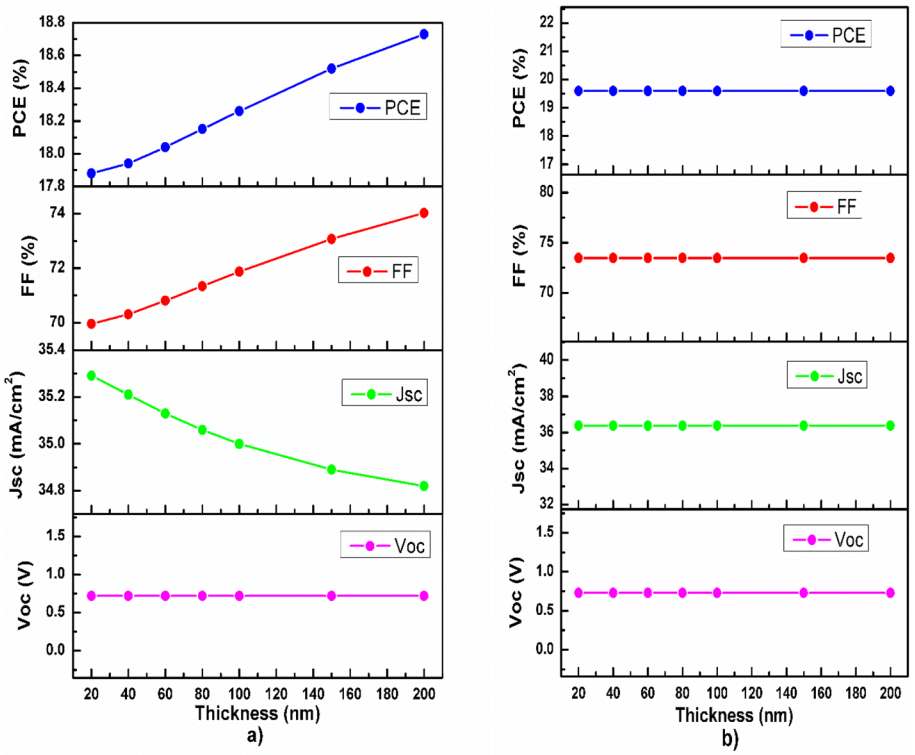

Fig. 8 Impact of n-GaAs ETL and P^+- CuO HTL thickness on the PV characteristics of studied heterostructure

revealed the possibility of achieving 16.62% efficiency with 1.2 µm Sb_2Se_3 layer thickness, 10^{15} cm^{-3} carrier concentration, 10^{13} cm^{-3} bulk defect, and 10^{10} cm^{-2} interface defect densities. Following this optimization study, we discovered that inserting n-GaAs (100 nm) at the n-CdS/p-Sb_2Se_3 interface and P^+-CuO HTL (100 nm) as a BSF increased the solar cell's efficiency even further. Furthermore, the inserted n-GaAs second buffer layer has been an important role in forming a positive CBO at the interface, allowing electron injection and diffusion from Sb_2Se_3 to CdS and thus increasing the device's yield. In addition, P^+-CuO HTL (BSF) was used to create a high barrier potential at the back contact, which reduces carrier recombination.

Finally, the ITO/CdS/GaAs/Sb_2Se_3/Au new solar cell achieves 19.60% efficiency, J_{sc} of 36.38 mA/cm^2, V_{oc} of 0.73 V, and FF of 73.47%, which will be encouraging to do experimental work on Sb_2Se_3 next-generation cost-efficient thin-film PV.

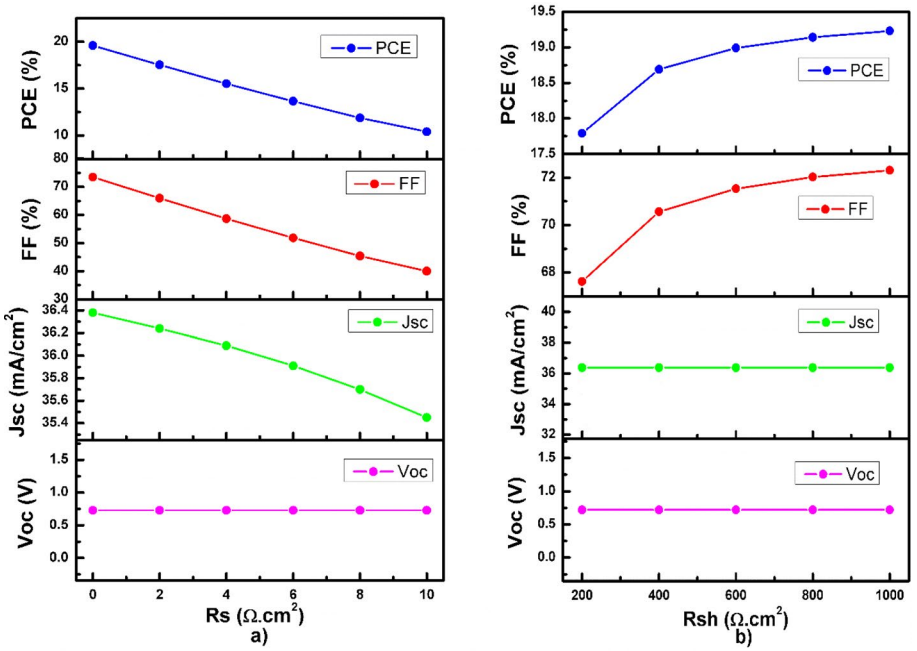

Fig. 9 the effect of Rs an Rsh parasitic resistance on the new PV hetero solar cell characteristics

Table 5 Comparative study of the current results and those found in the literature

Structure	Study type	Photovoltaic parameters				References
		J_{SC} (mA/cm^2)	V_{oc} (V)	FF (%)	η (%)	
Au/Sb_2Se_3/ CdS	Simulation	29.25	0.44	58.36	7.54	This work
Au/Sb_2Se_3/ CdS	Experimental	29.9	0.42	60.4	7.5	Wen et al. (2018)
Au/Sb_2Se_3/ CdS	Experimental	27.6	0.43	63.2	7.5	Yang et al. (2018)
Au/Sb_2Se_3/ CdS	Experimental	28.10	0.37	53.3	6.4	Tao et al. (2019)
Au/Sb_2Se_3/CdS	Optimized-1	35.38	0.66	70.33	16.62	This work
Au/Sb_2Se_3/CdS	Simulation	31.79	0.56	70.81	12.62	Basak and Singh (2021)
Au/CuO HTL/Sb_2Se_3/ GaAs/CdS	Optimized-2	36.38	0.73	73.47	19.60	This work
Au/CZTSe/Sb_2Se_3/ CdS	Simulation	34.66	0.66	81.18	18.50	Baig et al. (2020)

Acknowledgements The authors would like to thank Dr. Burgelman of Ghent University in Belgium for providing the SCAPS 1D simulation tool, as well as everyone else who contribute significantly to this scientific paper.

Authors' contributions The study's conception and design were contributed to by all of the authors. Material preparation, data collecting, and analysis were provided by Ph. D student AAA and Professor MS, while

Ph. D student EO, Professor *NK* and Professor AB provided feedback on the earlier manuscript. *The final paper was read and authorized by all of the writers.*

Funding The authors claim that they did not receive any funds, grants, or other forms of support while preparing this manuscript.

Data availability The data sources computed and analyzed during the present study are accessible upon reasonable request from the corresponding author (Abdelaziz AIT ABDELKADIR). All data investigated and analyzed in this original work research are included in this published paper as tables, figures, and detailed parameters with their reference's sources.

Declarations

Conflict of interest There are no detailed financials to specify for the authors.

Ethical approval Mr Abdelaziz AIT ABDELKADIR has approved the ethics of this study.

References

Abdelkadir, A.A., Oublal, E., Sahal, M., Gibaud, A.: Numerical simulation and optimization of n-Al-ZnO/n-CdS/p-CZTSe/p-NiO (HTL)/Mo solar cell System using SCAPS-1D. Results Opt. **8**, 100257 (2022a)

Abdelkadir, A.A., Sahal, M., Oublal, E., Kumar, N., Benami, A.: Performance enhancement investigations of the novel CZTGS thin-film solar cells. Opt. Mater. **133**, 112969 (2022b). https://doi.org/10.1016/j.optmat.2022.112969

Ait Abdelkadir, A., Oublal, E., Sahal, M., Soucase, B.M., Kotri, A., Hangoure, M., Kumar, N.: Numerical simulation and optimization of n-Al-ZnO/n-CdS/p-CIGS/p-Si/p-MoOx/Mo Tandem Solar Cell. SILICON (2022). https://doi.org/10.1007/s12633-022-02144-1

Baig, F., Khattak, Y.H., Shuja, A., Riaz, K., Soucase, B.M.: Performance investigation of Sb_2Se_3 based solar cell by device optimization, band offset engineering and Hole Transport Layer in SCAPS-1D. Curr. Appl. Phys. **20**, 973–981 (2020)

Basak, A., Singh, U.P.: Numerical modelling and analysis of earth abundant Sb2S3 and Sb2Se3 based solar cells using SCAPS-1D. Sol. Energy Mater. Sol. Cells **230**, 111184 (2021)

Biplab, S.R.I., Ali, M., Moon, M., Alam, M., Pervez, M., Rahman, M., Hossain, J.: Performance enhancement of CIGS-based solar cells by incorporating an ultrathin BaSi2 BSF layer. J. Comput. Electron. **19**, 342–352 (2020)

Burgelman, M., Marlein, J.: Analysis of graded band gap solar cells with SCAPS. In: Proc. Of the 23rd Eur. Photovolt. Sol. Energy Conf., Valencia. pp. 2151–2155 (2008)

Cang, Q., Guo, H., Jia, X., Ning, H., Ma, C., Zhang, J., Yuan, N., Ding, J.: Enhancement in the efficiency of Sb_2Se_3 solar cells by adding low lattice mismatch $CuSbSe_2$ hole transport layer. Sol. Energy **199**, 19–25 (2020)

Dong, J., Liu, Y., Wang, Z., Zhang, Y.: Boosting VOC of antimony chalcogenide solar cells: a review on interfaces and defects. Nano Select. **2**, 1818–1848 (2021)

Huang, M., Xu, P., Han, D., Tang, J., Chen, S.: Complicated and unconventional defect properties of the quasi-one-dimensional photovoltaic semiconductor Sb_2Se_3. ACS Appl. Mater. Interfaces. **11**, 15564–15572 (2019)

Kaminski, A., Vandelle, B., Fave, A., Boyeaux, J.P., Monna, R., Sarti, D., Laugier, A.: Aluminium BSF in silicon solar cells. Sol. Energy Mater. Sol. Cells **72**, 373–379 (2002)

Khan, A.D., Khan, A.D.: Optimization of highly efficient GaAs–silicon hybrid solar cell. Appl. Phys. A **124**, 1–10 (2018)

Khattak, Y.H., Baig, F., Toura, H., Beg, S., Soucase, B.M.: Efficiency enhancement of Cu_2BaSnS_4 experimental thin-film solar cell by device modeling. J. Mater. Sci. **54**, 14787–14796 (2019)

Oublal, E., Sahal, M., Abdelkadir, A.A.: New theoretical analysis of a novel hetero-junction SnS/CdS solar cell with homo-junction P-P+ in the rear face-numerical approach. Current Appl. Phys. **39**, 230–238 (2022)

Tang, R., Zheng, Z.-H., Su, Z.-H., Li, X.-J., Wei, Y.-D., Zhang, X.-H., Fu, Y.-Q., Luo, J.-T., Fan, P., Liang, G.-X.: Highly efficient and stable planar heterojunction solar cell based on sputtered and post-selenized Sb_2Se_3 thin film. Nano Energy **64**, 103929 (2019)

Tao, J., Hu, X., Xue, J., Wang, Y., Weng, G., Chen, S., Zhu, Z., Chu, J.: Investigation of electronic transport mechanisms in Sb_2Se_3 thin-film solar cells. Sol. Energy Mater. Sol. Cells **197**, 1–6 (2019)

Wen, X., Chen, C., Lu, S., Li, K., Kondrotas, R., Zhao, Y., Chen, W., Gao, L., Wang, C., Zhang, J.: Vapor transport deposition of antimony selenide thin film solar cells with 7.6% efficiency. Nat. Commun. **9**, 1–10 (2018)

Williams, R.E., Ramasse, Q.M., McKenna, K.P., Phillips, L.J., Yates, P.J., Hutter, O.S., Durose, K., Major, J.D., Mendis, B.G.: Evidence for self-healing benign grain boundaries and a highly defective Sb_2Se_3–CdS interfacial layer in Sb_2Se_3 thin-film photovoltaics. ACS Appl. Mater. Interfaces. **12**, 21730–21738 (2020)

Yang, X., Chen, B., Chen, J., Zhang, Y., Liu, W., Sun, Y.: ZnS thin film functionalized as back surface field in Si solar cells. Mater. Sci. Semicond. Process. **74**, 309–312 (2018)

Zhou, Y., Leng, M., Xia, Z., Zhong, J., Song, H., Liu, X., Yang, B., Zhang, J., Chen, J., Zhou, K.: Solution-processed antimony selenide heterojunction solar cells. Adv. Energy Mater. **4**, 1301846 (2014)